Journal of Molecular Structure xxx (xxxx) xxx

Contents lists available at ScienceDirect

Journal of Molecular Structure

journal homepage: www.elsevier.com/locate/molstr

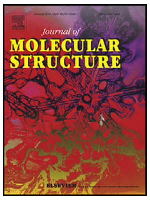

USY-zeolite catalyzed synthesis of 1,4-dihydropyridines under microwave irradiation: structure and recycling of the catalyst

Leonardo H.R. Alponti[a], Monize Picinini[b], Ernesto A. Urquieta-Gonzalez[b,*], Arlene G. Corrêa[a,*]

[a] Centre of Excellence for Research in Sustainable Chemistry, Department of Chemistry, Brazil
[b] Department of Chemical Engineering, Federal University of São Carlos, 13565-905 São Carlos, SP - Brazil

ARTICLE INFO

Article history:
Received 12 September 2020
Revised 6 October 2020
Accepted 7 October 2020
Available online xxx

Keywords:
multicomponent reaction
Green synthesis
Zeolite
Heterogenous catalysis
Microwave

ABSTRACT

The Hantzsch three-component reaction is the best-known multicomponent reaction, affording dihydropyridines which have been employed therapeutically and also as visible-light photoredox catalysts. In this work we report the application of an ultra-stable (US) Y zeolite as a promising green catalyst in the synthesis of a series of 1,4-dihydropyridines under microwave irradiation. Using the optimized reaction conditions, 21 compounds were prepared in 64-96% isolated yields. The recovery and recycle of the USY zeolite are also reported as well as its fully characterization.

1. Introduction

Important factors associated with the development of greener processes are atom economy, efficiency, elimination of toxic intermediates/products and generation of as minimum waste as possible [1]. In this sense, multicomponent reactions (MCRs) have emerged as an interesting tool that allows for the straightforward synthesis of intricate molecules in a one-pot fashion without the isolation and purification of intermediates, therefore leading to lower costs, time and energy consumption. Additionally, MCRs are modular and convergent in nature and also an important source of molecular diversity [2].

The 1,4-dihydropyridine synthesis using β-ketoesters, aldehydes and ammonia, reported by A. R. Hantzsch in 1881, is the best-known three-component reaction (3CR) [3]. This class of compounds has been extensively studied due to their potent biological activities [4]. Illustrative examples are nifedipine and nimodipine, that are employed therapeutically to reduce blood pressure and treat neurological deficits, respectively (Scheme 1). Hantzsch esters have also proven to be a useful class of electron donors and proton sources in photoredox catalyzed processes. Moreover, under photoredox catalytic conditions, alkyl-1,4-dihydropyridines can serve as versatile types of alkylation reagents via oxidative fragmentation mechanisms. The recent advances in the chemistry of Hantzsch esters in photoredox catalyzed organic synthesis have been reviewed [5].

Several mechanisms have been reported for the Hantzsch 3CR. Depending on the reaction conditions and substrates selected for the transformation, side reactions may take place in competition with the Hantzsch ester formation [6]. Due to its importance, literature survey discloses numerous synthetic protocols for 1,4-dihydropyridines synthesis [7], including green solvents such as water [8] or sodium acetate trihydrate–urea deep eutectic solvent (DES) [9], as well as solvent-free conditions [10], under infrared [11] or UV irradiation [12], microwave heating [13], and the use of citric acid as organocatalyst [14].

In the last decades, catalytic processes have unquestionably become a cornerstone within the Green Chemistry perspective, and their continuous advances have enabled the discontinuation of outdated stoichiometric methodologies to give place to more sustainable ones [15]. Among the major current challenges in this area is the replacement of conventional homogeneous catalysts by heterogeneous ones, which are easy to handle and usually recyclable, since they can be readily recovered. Recently, we have reviewed the applications of zeolites [16] as catalysts in multicomponent reactions [17].

The synthesis of 1,4-dihydropyridines using heterogeneous catalysis have been reported employing for example silica-supported sulphuric acid [18], silica gel/$NaHSO_4$ [19], sulfated zirconia [20], nano-crystalline solid acid catalyst [21], supported ionic

---

* Corresponding authors.
E-mail addresses: urquieta@ufscar.br (E.A. Urquieta-Gonzalez), agcorrea@ufscar.br (A.G. Corrêa).

https://doi.org/10.1016/j.molstruc.2020.129430

Please cite this article as: L.H.R. Alponti, M. Picinini, E.A. Urquieta-Gonzalez et al., USY-zeolite catalyzed synthesis of 1,4-dihydropyridines under microwave irradiation: structure and recycling of the catalyst, Journal of Molecular Structure, https://doi.org/10.1016/j.molstruc.2020.129430

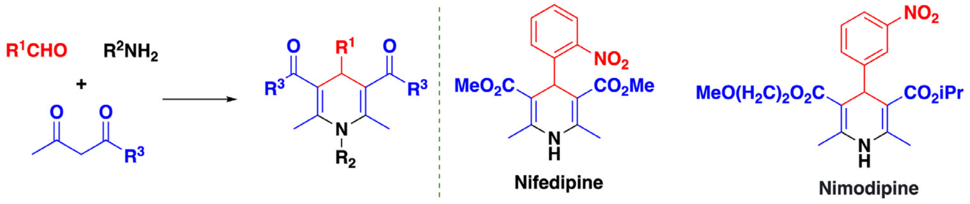

Scheme 1. The Hantzsch MCR and examples of dihydropyridines as commercially available drugs.

Table 1
Catalyst testing for 1,4-dihydropyridine synthesis.

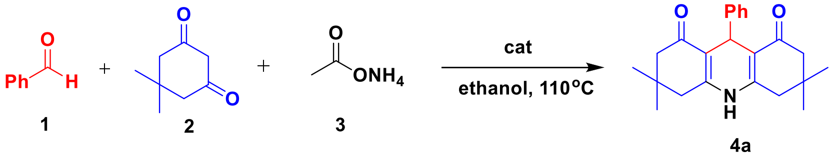

Entry[a]	Catalyst	Catalyst (mg)	Time (min)	**4a** yield (%)[b]
1	-	-	120	12
2	-	-	180	18
3	$CuCl_2.2H_2O$	3	120	70
4	$CuCl_2.2H_2O$	7	120	90
5	mordenite	100	120	82
6	ferrierite	100	120	87
7	ZSM-5	100	120	82
8	BETA	100	120	83
9	USY	100	120	96
10[c]	USY	100	10	96
11[c]	USY	100	15	95
12[c]	USY	50	15	82
13[c]	**USY**	**50**	**20**	**96**
14[c]	USY	25	20	63
15[c]	USY	25	25	71

[a] reactions were carried out using benzaldehyde **1** (0.5 mmol), dimedone **2** (1.0 mmol), ammonium acetate **3** (1.25 mmol) and EtOH (0.5 mL) in an oil bath at 110°C;
[b] isolated yield after column chromatography;
[c] performed under MW irradiation (110°C, 300 W).

liquid phase catalyst $[MerImi]PF_6$ under ultrasonication [22], and a negatively charged borotungstic acid $H_5BW_{12}O_{40}$ [23]. In this regard, zeolites, in particular, have received increasing attention owing to their efficiency and selectivity in organic transformations, as consequence of attractive properties, i.e. tunable acidity and pore size; still, an important feature of such materials is the possibility of inserting additional metals into their framework [24–26]. Nikpassand *et al*. reported the use of HY zeolite (Si/Al = 2.54) as catalyst for the Hantzsch synthesis using dimedone and 9 different aromatic aldehydes, under reflux of ethanol (2.5-3.5 h) [27]. The desired products were obtained in good yields (70-90%), although no information on the recycling of the catalyst was described.

Continuing our interest on the use of zeolites as green catalysts [28], in this work we report the promising application of an ultra-stable (US) Y zeolite in the synthesis of a series of 1,4-dihydropyridines.

2. Results and discussion

We initiated our study using dimedone, benzaldehyde, ammonium acetate in ethanol as solvent and evaluating different catalysts (Table 1) [29]. Through the data obtained in entries 1 and 2, it is possible to notice that the reaction needs a catalyst to intensify its performance. As copper has been reported to catalyze this reaction [30], we tested $CuCl_2.2H_2O$ (entries 3 and 4) and obtained product **4a** in good yields. However, aiming to develop more sustainable synthetic methods, a metal-free condition would be desired. Taking this into account, different zeolites, such as USY, ZSM-5 (Zeolite Socony Mobil – 5), ferrierite, mordenite and beta [31], having the Si/Al ratios shown in Table 2, where tested as catalyst in its protonic form in the described MCR at 110°C for 2 h using conventional heating (Table 1, entries 5-9).

As can be seen from Table 1, the USY zeolite showed to be the most suitable for the studied MCR, providing compound **4a** in 96% yield (entry 9). Looking for a more efficient protocol, microwave (MW) irradiation was tested, and for our delight, the desired product was still obtained on the USY zeolite in the same yield in only 10 min (entry 10). We then evaluated the catalyst loading (entries 12-15), using 50 or 25 mg of the USY zeolite under MW irradiation for 15, 20 or 25 min., and the best result was that of the entry 13, where the Hantzsch ester **4a** (Table 1), was isolated in 96% yield.

For the catalyst recycling study, the USY zeolite was separated from the reaction mixture and washed 4-5 times with ethanol followed by centrifugations for 5 min at 5000 W, and then reused. As shown in Fig. 1, the yield was still very good (> 90%) up to the 4th cycle.

The zeolites were characterized by XRD, SEM analyses and N_2 physisorption measurements. The XRD diffractograms of the zeolites in their protonic form, prepared as reported in previous works [32], confirmed its respective type FAU crystalline structure (Fig. 2a) [33]. Coherent with their crystal sizes of about 1 μm or higher (Fig. 3), the USY, mordenite, ferrierite and ZSM-5 zeolites present well resolved XRD patterns evidencing samples with high crystallinity (Fig. 4). The zeolite beta, constituted by agglomerates of nanosized crystals, generated a less resolved XRD pattern [34,35]. The textural properties of the studied zeolites

Table 2
Si/Al ratio and textural properties of the used zolites.

Zeolite	Si/Al[a]	Micropore[b] volume ($cm^3 \cdot g^{-1}$)	External[b] surface area ($m^2 \cdot g^{-1}$)	Structure, Micropore system and pore diameter[c] (nm)
mordenite	10	0.159	53.4	MOR 1D–12/8-ring 0.71 × 0.62 / 0.48 × 0.38
ferrierite	10	0.118	39.3	FER 2D–10/8-ring 0.42 × 0.54 / 0.35 × 0.48
ZSM-5	20	0.159	24.4	MFI 3D–10-ring 0.56 × 0.53 / 0.55 × 0.51
Beta	15	0.160	228	BEA 3D–12-ring 0.66 × 0.77 / 0.56 × 0.56
USY	2.9	0.273	22.9	FAU 3D–12-ring 0.74

[a] Si/Al ratio determined by EDX;
[b] Calculated using the t-plot method [39];
[c] Data from the International Zeolite Association [40].

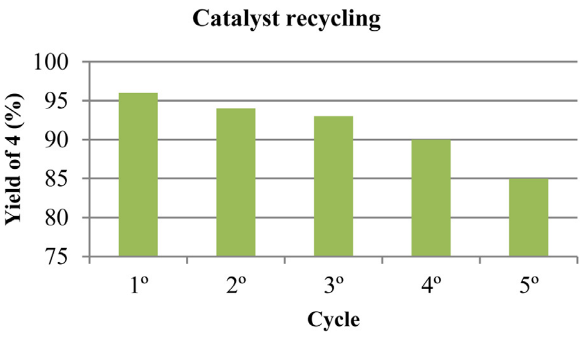

Fig. 1. Yield of compound **4a** for each reaction cycle using the USY zeolite as catalyst.

(Table 2) clearly show a superior microporous volume for the USY zeolite.

In order to better understanding its role of as heterogeneous catalyst in the Hantzsch 3CR, the USY zeolite was also analysed by *in situ* FTIR of adsorbed pyridine. The obtained results showed that besides its 3D microporous structure [31] (Table 2) and the above commented higher microporous volume (Table 2) and high specific surface area (Table 3), the acidic nature of the USY active sites (Table 3), was another important contributing factor on its best catalytic behavior [37]. In this way, the USY zeolite, because its lower Si/Al ratio, shows a high amount of active acid sites with Brønsted nature (Fig. 2b and Table 3) [38].

Moreover, the high stability of the USY zeolite as catalyst is demonstrated by XRD (Fig. 2a), textural (Table 3), and *in situ* FTIR of adsorbed pyridine (Fig. 2b and Table 3) data, which were

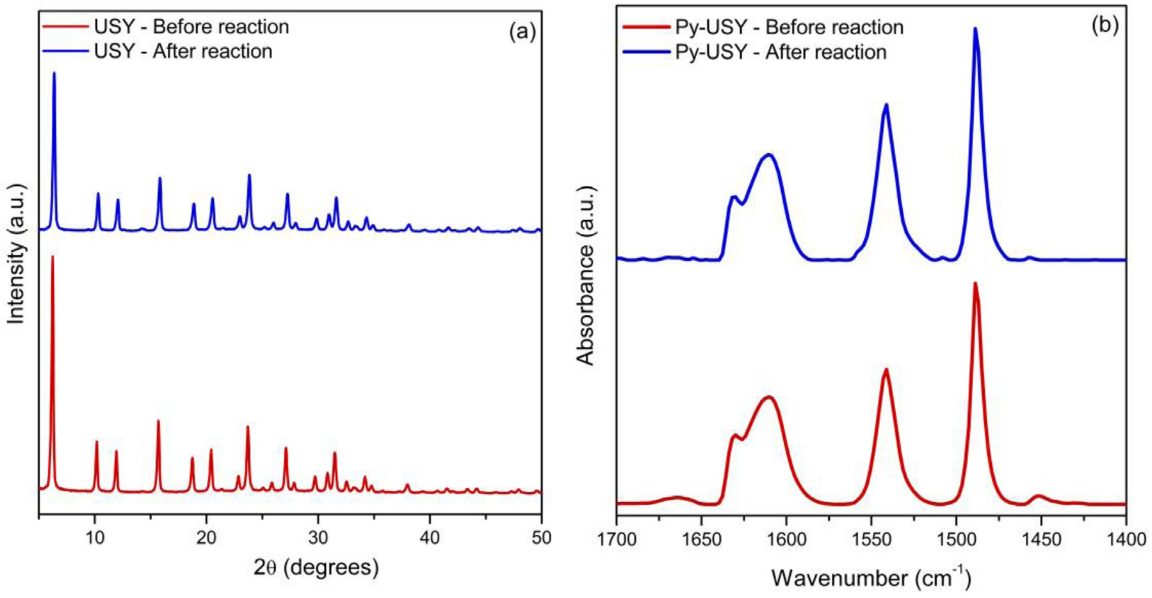

Fig. 2. Fresh USY zeolite (in red) and USY zeolite recovered from the reaction mixture (in blue): (a) XRD diffractograms; (b) *in-situ* DRIFTS spectra of adsorbed pyridine [36]. Brønsted acid sites band at ~1545 cm^{-1}, Lewis acid sites band at ~1450 cm^{-1}.

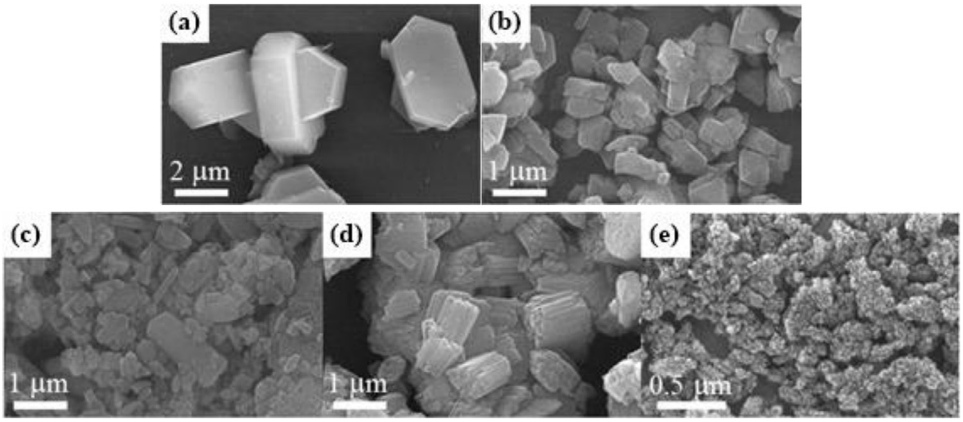

Fig. 3. SEM micrograph of the used commercial zeolites: (a) ZSM-5; (b) USY; (c) ferrierite; (d) mordenite; (e) beta.

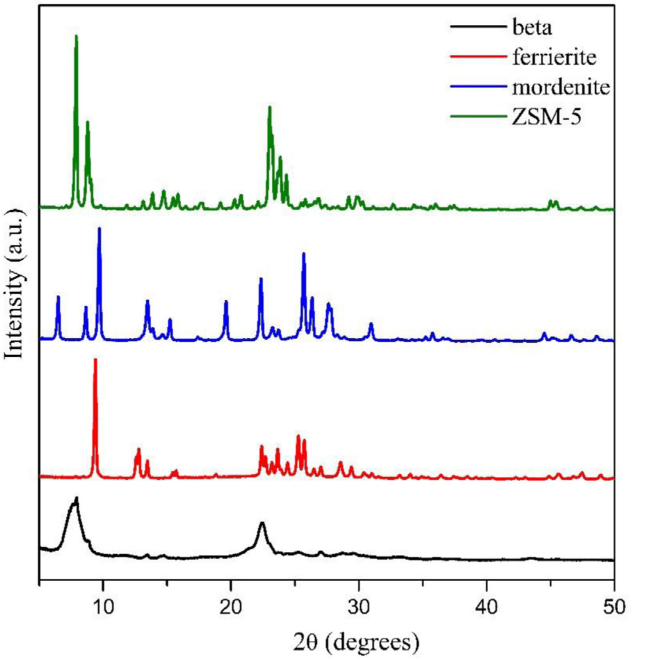

Fig. 4. XRD diffractograms of the used protonic beta, ferrierite, mordenite and ZSM-5 zeolites.

Table 3
Textural and acid properties of the USY zeolite.

Sample	[1]BET area ($m^2.g^{-1}$)	[2]$C_{Brønsted}$ ($\mu mol.g^{-1}$)	[3]C_{Lewis} ($\mu mol.g^{-1}$)
[4]USY_{fresh}	679	446	<15
[5]USY_{spent}	669	482	<15

[1] Specific surface area;
[2] Brønsted acid sites;
[3] Lewis acid sites
[4] Before reaction;
[5] After reaction.

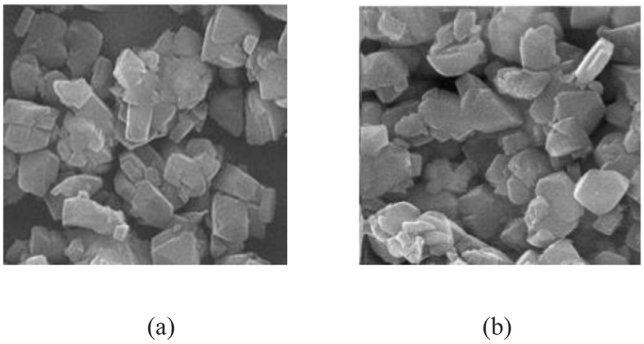
(a) (b)

Fig. 5. MEV images showing the USY zeolite: (a) before (fresh) and (b) after (spent) reaction.

obtained before (fresh USY) and after (spent USY) reaction. As can be evidenced, the FAU structure (Fig. 2a), the specific surface area (Table 3) and acidic properties (Table 3 and Fig. 2b), of the fresh USY zeolite are practically preserved after reaction (spent USY zeolite). As can be seen in Fig. 5, coherently with the commented XRD and acidic properties stability, MEV images did not show any changes in the original morphology of the USY zeolite.

We then turned our attention for the evaluation of the scope and limitation of this method using different aldehydes and dimedone or ethyl acetoacetate. As can be observed on Table 4, in general the best yields were obtained with dimedone probably due to its higher acidity. It is worth to mention that pentan-2,4-dione and heptan-3,5-dione have been tested as well, however the desired products were not obtained recovering the starting material. Aromatic aldehydes containing both electron donor and withdrawing groups were successfully employed furnishing good to excellent isolated yields (entries 1-4), excepting for 4-nitrobenzaldehyde as only traces of the desired product was observed (entry 5). In order to obtain compounds **4e** and **4o**, we have also tested the reactions under MW irradiation at 90 and 100 °C without success. When aliphatic aldehydes were tested, once again the corresponding 1,4-dihydropyridines were obtained in good yields (entries 6-8), including the new derivative **4h**. Furthermore, heteroaromatic aldehydes could also be employed affording the corresponding products in good yields (entries 9-10). Finally, we have tested this protocol in the synthesis of acridinediones using *p*-toluidine instead of ammonium acetate [16], and for our delight the desired product **5** was obtained in 64% isolated yield (Scheme 2).

Table 4
Scope of the three-component reaction catalyzed by USY zeolite.

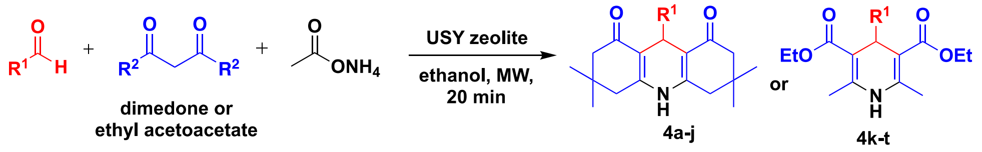

Entry[a]	Aldehyde (R^1)	Yield (%)[b] with dimedone	Yield (%)[b] with ethyl acetoacetate
1	C_6H_5	**4a**, 96	**4k**, 90
2	$4\text{-}CH_3OC_6H_4$	**4b**, 95	**4l**, 83
3	$3\text{-}BrC_6H_4$	**4c**, 83	**4m**, 75
4	$4\text{-}NCC_6H_4$	**4d**, 83	**4n**, 78
5	$4\text{-}NO_2C_6H_4$	**4e**, traces	**4o**, traces
6	C_6H_{11}	**4f**, 87	**4p**, 62
7	$(CH_2)_6CH_3$	**4g**, 72	**4q**, 64
8	$(CH_2)_8CH_3$	**4h**, 80	**4r**, 60
9	C_4H_4S	**4i**, 88	**4s**, 88
10	NC_5H_4	**4j**, 85	**4t**, 85

[a] All reactions were performed using aldehyde (0.5 mmol), diketone (1.0 mmol), ammonium acetate (1.25 mmol), USY zeolite (50 mg) and EtOH (0.5 mL) under MW irradiation (110°C, 300 W) for 20 min.

[b] Isolated yield after column chromatography.

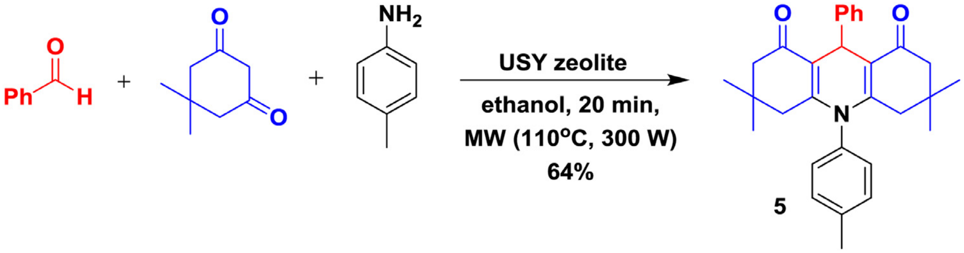

Scheme 2. Synthesis of acridinedione 5.

3. Conclusion

In conclusion we report herein the promising application of an USY zeolite as a green catalyst in the synthesis of a series of 1,4-dihydropyridines under microwave irradiation. After simple recovery, the USY zeolite could be reused up to the 4th cycle still furnishing excellent isolated yield (> 90%) of compound **4a**. The USY zeolite was fully characterized in order to better understanding its catalytic stability and its role of as heterogeneous catalyst. The best catalytic behavior of the USY zeolite was attributed to its microporous structure and their textural and acidic properties. Using such USY zeolite and optimized reaction conditions, 21 compounds were prepared in 64-96% isolated yields.

4. Experimental section

4.1. Zeolites characterization

The zeolites used in this study were prepared as reported in previous works [32], and only one batch of each catalyst has been used. The X-ray diffractograms of the used zeolites were collected between 5 and 50° (2θ) with a step-rate of 10° (2θ) min^{-1}, using a Rigaku Miniflex diffractometer operated with Cu Kα radiation ($\lambda = 1.5418$ Å) at 40 kV and 30 mA. The specific surface area (BET) of the USY zeolite was obtained from N_2 physisorption data at -196°C using a Micromeritics ASAP-2020 apparatus. Prior to the analysis, the zeolite was degassed for 5 h at 300°C under a vacuum of 20 µmHg. The micropores volume and the external specific surface area were estimated using the *t*-plot method, assuming the Harkins–Jura thickness equation [41]. Taking into consideration the criteria recommended by IUPAC [42], values of the apparent BET surface area at $P/P_0=0.95$ of the fresh and spent USY zeolite were determined. The morphological characteristics and the Si/Al ratio of the zeolites were determined by scanning electron microscopy with energy-dispersive X-ray spectroscopy (SEM-EDX) using a FEI Magellan 400L electronic microscope.

Analyses of *in-situ* FTIR of adsorbed pyridine were used to investigate the nature of the acid sites (Brønsted and Lewis) of the fresh and spent USY zeolites [43]. The measurements were performed using a high-temperature cell (Harrick) and a Bruker Vertex 70 spectrometer equipped with a mercury cadmium telluride detector. Prior to the measurement, the analyzed sample was pretreated at 350°C for 1 h under an argon flow (60 mL min^{-1}) and then cooled to 150°C. Afterward, the sample was saturated by pulses of pyridine vapor. The excess and the weakly adsorbed pyridine on the zeolite surface were purged with an argon flow (60 mL min^{-1}) for 2 h. Finally, the sample was analyzed in the region from 1700 to 1400 cm^{-1} with a nominal resolution of 4 cm^{-1} and accumulation of 180 scans. All the spectra of adsorbed pyridine were collected at 150°C and removed from the spectrum of the zeolite before adsorption. A reference spectrum was acquired for dried KBr, under the same conditions. The concentration of Brønsted and Lewis acid sites was estimated using the equations $C_{\text{Brønsted}} = AB/(\varepsilon B^*\alpha)$ and $C_{\text{Lewis}} = AL/(\varepsilon L^*\alpha)$, where AB and AL are the areas of the bands at around 1545 cm^{-1} (pyridinium ions bonded to Brønsted acid sites) and 1450 cm^{-1} (pyridine coordinated to Lewis acid sites), respectively; εL (1.73 cm μmol^{-1}) and εB (1.23 cm μmol^{-1}) are the extinction coefficients related to the Lewis and Brønsted acid sites [39], respectively; and α is the ratio of the sample mass to the pellet area.

4.2. Synthesis of 1,4-dihydropyridines

The commercially available reagents were purchased from Sigma-Aldrich or Alfa Aesar and, when necessary, treated according to the procedures described in the literature. The purification of the products was performed by a flash chromatographic column, using silica gel 60, 230-400 mesh ASTM Merck and silica gel 60 A, 70-230 mesh AldrichCo. The thin layer chromatography analyses were carried out on silica gel 60 F254 plates supported on aluminum sheets and developed under ultraviolet light and / or stained in an acid vanillin. The solvent excess was evaporated in Buchi Rotavapor R-114 with BuchiWatherbath B-490 bath. The Nuclear Magnetic Resonance spectra (^{1}H and ^{13}C NMR) were recorded on the Bruker ARX 400 MHz spectrometers. The chemical shifts (δ) are expressed in ppm and the coupling constants (J) in Hertz (Hz). To indicate the multiplicity of signs, the following abbreviation was used: s (singlet), d (doublet), dd (double doublet), t (triplet), m (multiplet). Mass Spectra were recorded on a Shimadzu GCMS-QP5000. The reactions using microwaves were performed using a CEM Discovery equipment making use of the equipment's cooling system in all reactions.

4.2.1. General procedure

In a sealed tube, a mixture of diketone or β-ketoester (1.0 mol), aldehyde (0.5 mol) and ammonium acetate or *p*-toluidine (1.25 mol) was carried out with the zeolite catalyst USY (50 mg) at 0.5 mL of ethanol, heated to 110°C (300 W) in an oil bath or under microwave irradiation (300 W) for the time required for product formation. The progress of the synthesis was verified by TLC. After completing the time proposed in the optimization of the reaction, the reaction mixture was diluted with ethanol (5-6 mL) and the catalyst was separated by centrifugation, along 3 processes followed by washing of the mixture composed of the desired product diluted in ethanol and the heterogeneous catalyst, this solvent being eliminated by vacuum, resulting in a solid that was purified by column chromatography using hexane / ethyl acetate as eluent.

For the catalyst recycling study, the zeolite was separated from the reaction mixture and washed 4-5 times with ethanol followed by centrifugations for 5 min at 5000 W. At the end of each washing process, the zeolite was placed in the kiln to remove the remaining ethanol and then weighed to be reused. In all cycles the catalyst was practically fully recovered, that is, in all syntheses it was possible to use approximately 50 mg of USY zeolite.

4.2.2. Compounds characterization

*3,3,6,6-tetramethyl-9-phenyl-3,4,6,7,9,10-hexahydroacridine-1,8(2H,5H)-dione (**4a**)* [8]:

Light yellow solid (0.167g, 96%), m.p.190-192°C. ^{1}H NMR ($CDCl_3$, 400 MHz, ppm) δ 8.00 (bs, 1H), 7.33 (d, J = 7.8 Hz, 2H), 7.18 (t, J = 7.4 Hz, 2H), 7.06 (t, J = 7.2 Hz, 1H), 5.08 (s, 1H), 2.32-2.10 (m, 8H), 1.05 (s, 6H), 0.94 (s, 6H).

*9-(4-methoxyphenyl)-3,3,6,6-tetramethyl-3,4,6,7,9,10-hexahydroacridine-1,8(2H,5H)-dione (**4b**)* [10b]:

Light yellow solid (0.180g, 95%), m.p. 270-272°C. ^{1}H NMR ($CDCl_3$, 400 MHz, ppm) δ 7.96 (bs, 1H), 7.22-7.26 (m, 2H), 6.71 (d, J = 8.4 Hz, 2H), 5.03 (s, 1H), 3.66 (s, 3H), 2.11-2.27 (m, 8H), 1.05 (s, 6H), 0.94 (s, 6H).

*9-(3-bromophenyl)-3,3,6,6-tetramethyl-3,4,6,7,9,10-hexahydroacridine-1,8 (2H,5H)-dione (**4c**)* [8]:

Light yellow solid (0.170g, 83%), m.p. 286-288°C. ^{1}H NMR ($CDCl_3$, 400 MHz, ppm) δ 7.44 (bs, 1H), 7.35 (bs, 1H), 7.25 (d, J = 7.6 Hz, 1H), 7.14 (d, J = 7.7 Hz, 1H), 7.00 (t, J = 7.8 Hz, 1H), 4.98 (s, 1H), 2.28-2.18 (m, 4H), 2.18–2.06 (m, 4H), 1.01 (s, 6H), 0.91 (s, 6H).

*4-(3,3,6,6-tetramethyl-1,8-dioxo-1,2,3,4,5,6,7,8,9,10-decahydroacridin-9-yl) benzonitrile (**4d**)* [14]:

Light yellow solid (0.155g, 83%), m.p. 298-300°C. ^{1}H NMR ($CDCl_3$, 400 MHz, ppm) δ 7.47 (dd, J = 18.6, 8.0 Hz, 4H), 6.00 (bs, 1H), 5.03 (s, 1H), 2.40-2.16 (m, 8H), 1.03 (s, 6H), 0.89 (s, 6H).

*9-cyclohexyl-3,3,6,6-tetramethyl-3,4,6,7,9,10-hexahydroacridine-1,8(2H,5H)-dione (**4f**)* [12]:

Light yellow solid (0.154g, 87%), m.p. 249-251°C. ^{1}H NMR ($CDCl_3$, 400 MHz, ppm) δ 6.95 (bs, 1H), 4.05 (s, 1H), 2.42-2.20 (m, 9H), 1.62 (t, J = 14.8 Hz, 5H), 1.40-1.19 (m, 3H), 1.14 (s, 6H), 1.09 (s, 6H), 0.91-0.81 (m, 2H).

*3,3,6,6-tetramethyl-9-heptyl-3,4,6,7,9,10-hexahydroacridine-1,8(2H,5H)-dione (**4g**)* [8]:

Yellow solid (0.133g, 72%), m.p. 109-111°C. ^{1}H NMR ($CDCl_3$, 400 MHz, ppm) δ 7.63 (s, 1H), 4.06 (t, J = 4.9 Hz, 1H), 2.42-2.19 (m, 8H), 1.44-1.14 (m, 12H), 1.10 (s, 6H), 1.09 (s, 6H), 0.82 (t, J = 6.8 Hz, 3H).

*3,3,6,6-tetramethyl-9-nonyl-3,4,6,7,9,10-hexahydroacridine-1,8(2H,5H)-dione (**4h**)*:

Yellow solid (0.159g, 80%), m.p. 134-137°C. ^{1}H NMR ($CDCl_3$, 400 MHz, ppm) δ 7.06 (bs, 1H), 4.07 (t, J = 4.8 Hz, 1H), 2.37-2.23 (m, 8H), 1.44-1.16 (m, 16H), 1.10 (s, 6H), 1.09 (s, 6H), 0.87 (t, J = 6.8 Hz, 3H). ^{13}C NMR (101 MHz; $CDCl_3$) δ 196.1, 149.8, 112.7, 51.0, 41.1, 35.1, 32.5, 31.9, 30.0, 29.7, 29.7, 29.6, 29.3, 27.2, 27.1, 25.4, 22.7, 14.1. GC-MS (70 eV) *m/z* (%): 434.4 (100), 406.3, 398.3, 339.1, 325.1, 311.2.

*3,3,6,6-tetramethyl-9-(thiophen-2-yl)-3,4,6,7,9,10-hexahydroacridine-1,8 (2H,5H)-dione (**4i**)* [9]:

Light orange solid (0.155g, 80%); m.p. 284-286°C. ^{1}H NMR ($CDCl_3$, 400 MHz, ppm) δ 6.98 (d, J = 4.9 Hz, 1H), 6.92 (d, J = 3.1 Hz, 1H), 6.83-6.80 (m, 1H), 6.12 (bs, 1H), 5.40 (s, 1H), 2.37-2.25 (m, 8H), 1.10 (s, 6H), 1.04 (s, 6H).

*3,3,6,6-tetramethyl-9-(pyridin-2-yl)-3,4,6,7,9,10-hexahydroacridine-1,8 (2H,5H)-dione (**4j**)* [9]:

Light orange solid (0.148g, 85%), m.p. 299-301°C. ^{1}H NMR ($CDCl_3$, 400 MHz, ppm) δ 8.81 (d, J = 4.6 Hz, 1H), 7.61 (d, J = 7.7 Hz, 1H), 7.54 (t, J = 7.6 Hz, 1H), 7.01-6.96 (m, 1H), 6.55 (bs, 1H), 5.20 (s, 1H), 2.35-2.15 (m, 8H), 1.07 (s, 6H), 0.98 (s, 6H).

*Diethyl-2,6-dimethyl-4-phenyl-1,4-dihydropyridine-3,5-dicarboxylate (**4k**)* [44]:

Light yellow solid (0.168g, 90%), m.p. 155-157°C. ^{1}H NMR ($CDCl_3$, 400 MHz, ppm) δ 7.24 (d, J = 1.9 Hz, 2H), 7.17 (t, J = 7.4 Hz, 2H), 7.09 (t, J = 7.2 Hz, 1H), 5.58 (bs, 1H), 4.96 (s, 1H), 4.10-4.01 (m, 4H), 2.30 (s, 6H), 1.19 (t, J = 7.1 Hz, 6H).

*Diethyl-4-(4-methoxyphenyl)-2,6-dimethyl-1,4-dihydropyridine-3,5-dicarboxylate (**4l**)* [21]:

Light yellow solid (0.148g, 83%); m.p. 164-166°C. ^{1}H NMR ($CDCl_3$, 400 MHz, ppm) δ 7.19 (d, J = 8.0 Hz, 2H), 6.74 (d, J = 8.1 Hz, 2H), 5.70 (bs, 1H), 4.92 (s, 1H), 4.13-4.04 (m, 4H), 3.74 (s, 3H), 2.31 (s, 6H), 1.22 (t, J = 7.1 Hz, 6H).

*Diethyl-4-(3-bromophenyl)-2,6-dimethyl-1,4-dihydropyridine-3,5-dicarboxylate (**4m**)* [44]:

Yellow solid (0.153g, 75%), m.p. 112-114°C. ^{1}H NMR ($CDCl_3$, 400 MHz, ppm) δ 7.45 (bs, 1H), 7.35-7.29 (m, 2H), 7.07 (t, J = 7.8 Hz, 1H), 5.98 (s,1H), 4.94 (s, 1H), 4.12-4.05 (m, 4H), 2.31 (s, 6H), 1.21 (t, J = 6.8 Hz, 6H).

Diethyl-4-(4-cyanophenyl)-2,6-dimethyl-1,4-dihydropyridine-3,5-dicarboxylate (**4n**) [21]:

Brown solid (0.138g, 78%); m.p. 192-194°C. ^{1}H NMR ($CDCl_3$, 400 MHz, ppm) δ 7.50 (d, J = 7.8 Hz, 2H), 7.39 (d, J = 7.6 Hz, 2H), 5.80 (bs, 1H), 5.03 (s, 1H), 4.12-4.04 (m, 4H), 2.34 (s, 6H), 1.20 (t, J = 7.1 Hz, 6H).

*Diethyl-4-cyclohexyl-2,6-dimethyl-1,4-dihydropyridine-3,5-dicarboxylate (**4p**)* [44]:

Orange solid (0.100g, 60%); m.p. 112-114°C. ^{1}H NMR ($CDCl_3$, 400 MHz, ppm) δ 5.61(bs,1H), 4.23–4.12 (m, 4H), 3.91 (d, J=5.4 Hz, 1H); 2.29 (s, 6H), 1.54 (d, J = 12.0 Hz, 4H), 1.29 (t, J =7.1 Hz, 9H), 1.06 (d, J =7.2 Hz, 4H).

*Diethyl-4-heptyl-2,6-dimethyl-1,4-dihydropyridine-3,5-dicarboxylate (**4q**)* [45]:

Orange oil (0.112g, 64%). ^{1}H NMR ($CDCl_3$, 400 MHz, ppm) δ 5.62 (bs, 1H), 4.23-4.11 (m, 4H), 3.91 (t, J = 5.8 Hz, 1H), 2.27 (s, 6H), 1.35-1.25 (m, 12H), 1.20 (bs, 6H), 0.85 (t, J = 7.0 Hz, 3H).

*Diethyl-2,6-dimethyl-4-nonyl-1,4-dihydropyridine-3,5-dicarboxylate (**4r**)* [46]:

Orange oil (0.113g, 60%). ^{1}H NMR (CDCl$_3$, 400 MHz, ppm) δ 5.85-5.75 (m, 1H), 4.20-4.09 (m, 4H), 3.89 (t, $J = 5.7$ Hz, 1H), 2.25 (s, 6H), 1.30-1.22 (m, 12H), 1.21 (bs, 10H), 0.85 (t, $J = 5.6$ Hz, 3H).

*Diethyl-2,6-dimethyl-4-(thiophen-2-yl)-1,4-dihydropyridine-3,5-dicarboxylate (**4s**)* [21]:

Light yellow solid (0.147g, 88%); m.p. 170-172°C. ^{1}H NMR (CDCl$_3$, 400 MHz, ppm) δ 7.04 (d, $J = 5.0$ Hz, 1H), 6.84 (t, $J = 4.2$ Hz, 1H), 6.79 (d, $J = 3.3$ Hz, 1H), 5.88 (bs, 1H), 5.34 (s, 1H), 4.25-4.08 (m, 4H), 2.33 (s, 6H), 1.27 (t, $J = 7.0$ Hz, 6H).

*Diethyl-2,6-dimethyl-4-(2-pyridyl)-1,4-dihydropyridine-3,5-dicarboxylate (**4t**)* [22]:

Brown solid (0.140g, 85%); m.p. 194-196°C. ^{1}H NMR (CDCl$_3$, 400 MHz, ppm) δ 9.03 (d, $J = 13.3$ Hz, 1H), 8.47 (d, $J = 4.8$ Hz, 1H), 7.58 (t, $J = 7.6$ Hz, 1H), 7.40 (d, $J = 7.8$ Hz, 1H), 7.16-7.11 (m, 1H), 5.18 (s, 1H), 4.04 (q, J = 7.0 Hz, 4H), 2.22 (s, 6H), 1.18 (t, $J = 7.1$ Hz, 6H).

*3,3,6,6-tetramethyl-9-phenyl-10-(p-tolyl)-3,4,6,7,9,10-hexahydroacridine-1,8(2H,5H)-dione (**5**)* [18]:

Orange solid (0.140g, 64%); m.p.265-267 °C. ^{1}H NMR (CDCl$_3$, 400 MHz, ppm) δ 7.28 (d, $J = 4.2$ Hz, 2H), 7.21 (t, $J = 7.5$ Hz, 2H), 7.10 (t, $J = 7.2$ Hz, 1H), 6.97 – 6.90 (m, 2H), 6.71 (d, $J = 8.0$ Hz, 2H), 5.26 (s, 1H), 2.47 – 2.18 (m, 11H), 1.11 (s, 6H), 1.01 (s, 6H).

Declaration of Competing Interest

There are no conflicts to declare.

CRediT authorship contribution statement

Leonardo H.R. Alponti: Conceptualization, Methodology. **Monize Picinini:** Investigation, Formal analysis. **Ernesto A. Urquieta-Gonzalez:** Supervision, Writing - original draft. **Arlene G. Corrêa:** Supervision, Writing - review & editing.

Acknowledgements

The authors gratefully acknowledge FAPESP (grants 2013/07600-3, 2014/50249-8 and 2018/12367-0), GlaxoSmithKline, CAPES (Finance Code 001), and CNPq (grant 429748/2018-3 and 302140/2019-0) for funding and fellowships.

Supplementary materials

Supplementary material associated with this article can be found, in the online version, at doi:10.1016/j.molstruc.2020.129430.

References

[1] R.A. Sheldon, Green Chem. 19 (2017) 18–43.
[2] D. Das, Chemistry Select 1 (2016) 1959–1980.
[3] (a) A. Saini, S. Kumar, J.S. Sandhu, J. Sci. Ind. Res. 67 (2008) 95–111; (b) F. Bossert, H. Meyer, E. Wehinger, Angew. Chem. Int. Ed. 20 (1981) 762–769.
[4] S. Sepehri, H.P. Sanchez, A. Fassihi, J. Pharm. Pharmac. Sci. 18 (2015) 1–52.
[5] P.-Z. Wang, J.-R. Chen, W.-J. Xiao, Org. Biomol. Chem. 17 (2019) 6936–6951.
[6] H.G.O. Alvim, E.N. da Silva Júnior, B.A.D. Neto, RSC Adv. 4 (2014) 54282–54299.
[7] (a) S. Farooq, M.A. Munawar, Z. Ngani, Curr. Org. Chem. 22 (2018) 2671–2680; (b) L.L. Lu, H. Xu, P. Zhou, F.C. Yu, Chin. J. Org. Chem. 36 (2016) 2858–2879; (c) D.M. Stout, A.I. Meyers, Chem. Rev. 82 (1982) 223–243.
[8] K.N. Tiwari, M.R. Uttam, P. Kumari, P. Vatsa, S.M. Prabhakaran, Synth. Commun. 47 (2017) 1013–1019.
[9] C.A. Navarro, C.A. Sierra, C. Ochoa-Puentes, RSC Adv. 6 (2016) 65355–65365.
[10] (a) M.A. Zolfigol, M. Safaiee, Synlett 5 (2004) 827–828; (b) Y.-S. Bing, G.-W. Wang, Arkivoc 16 (2008) 1–8.
[11] R. Osnaya, G.A. Arroyo, L. Parada, F. Delgado, J. Trujillo, M. Salmón, R. Miranda, Arkivoc 11 (2003) 112–117.
[12] C.M. Kormos, R.M. Hull, N.E. Leadbeater, Aust. J. Chem. 62 (2009) 51–57.
[13] (a) L. Ohberg, J. Westman, Synlett 8 (2001) 1296–1298; (b) S.K. Singh, K.N. Singh, J. Heterocycl. Chem. 48 (2010) 69–73; (c) J.C. Legay, E.J.J. Vanden, J.P. Bazureau, Tetrahedron 61 (2005) 12386–12397.
[14] M. Patil, S. Karhale, A. Kudale, A. Kumbhar, S. More, V. Helavi, Curr. Sci. 6 (2019) 936–942.
[15] R.A. Sheldon, J. R. Soc. Interface 13 (2016) 20160087.
[16] J. Cejka, H. van Bekkum, A. Corma, F. Schüth, Introduction to Zeolite Science and Practice (Studies in Surface Science and Catalysis), 168, 3rd ed, Elsevier Science, 2007.
[17] C.G.S. Lima, N.M. Moreira, M.W. Paixão, A.G. Corrêa, Curr. Opin. Green Sustain. Chem. 15 (2019) 7–12.
[18] S.S. Mansoor, K. Aswin, K. Logaiya, S.P.N. Sudhan, J. Taibah. Univ. Sci. 8 (2014) 265–275.
[19] M.A. Chari, K. Syamasundar, Catal. Commun. 6 (2005) 624–626.
[20] D. Angeles-Beltrán, L. Lomas-Romero, V.H. Lara-Corona, E. González-Zamora, G. Negrón-Silva, Molecules 11 (2006) 731–738.
[21] A. Teimouri, L. Ghorbanian, A. Moatari, Bull. Chem. Soc. Ethiopia 27 (2013) 427–438.
[22] M. Jagadale, D. Kale, R. Salunkhe, M. Rajmane, G. Rashinkar, J. Molec. Liq. 265 (2018) 525–535.
[23] T. Momeni, M.M. Heravi, T. Hosseinnejad, M. Mirzaei, V. Zadsirjan, J. Mol. Struct. 1199 (2020) 127011.
[24] T. Ennaert, J. Van Aelst, J. Dijkmans, R. De Clercq, W. Schutyser, M. Dusselier, D. Verboekend, B.F. Sels, Chem. Soc. Rev. 45 (2016) 584–611.
[25] F.-S. Xiao, X. Meng, Zeolites in Sustainable Chemistry, 1st ed, Springer, Heidelberg, 2016.
[26] R. Srivastava, Catal. Today 309 (2018) 172–188.
[27] M. Nikpassand, M. Mamaghani, K. Tabatabaeian, Molecules 14 (2009) 1468–1474.
[28] (a) E. Jorge, T.M. Lima, C.G.S. Lima, L. Marchini, W.N. Castelblanco, D.G. Rivera, E.A. Urquieta-González, R.S. Varma, M.W. Paixão, Green Chem. 19 (2017) 3856–3868; (b) T.M. Lima, C.G.S. Lima, A.K. Rathi, M.B. Gawande, J. Tuce, E.A. Urquieta-González, R. Zbořil, M.W. Paixão, R.S. Varma, Green Chem. 18 (2016) 5586–5593.
[29] G. Busca, Micropor. Mesopor. Mat. 254 (2017) 3–16.
[30] (a) M.G. Dekamin, E. Kazemi, Z. Karimi, M. Mohammadalipoor, M.R. Naimi-Jamal, Int. J. Biol. Macromol. 93 (2016) 767–774; (b) K.K. Pasunooti, C.N. Jensen, H. Chai, M.L. Leow, D.W. Zhang, X.W. Liu, J. Comb. Chem. 12 (2010) 577–581.
[31] C.H. Baerlocher, L.B. McCusker, D.H. Olson, Atlas of Zeolite Framework Types, 6th edition, Elsevier, Amsterdam, 2007.
[32] (a) D.S. Ferracine, E. D., K.T.G. Carvalho, D.S.A. Silva, E.A. Urquieta-Gonzalez, Catal. Lett. (2020), doi:10.1007/s10562-020-03262-4; (b) K.T.G. Carvalho, D.S. Araújo Silva, E.A. Urquieta-Gonzalez, Ind. Eng. Chem. Res. 58 (2019) 7044–7051, doi:10.1007/s10562-020-03262-4.
[33] M.M.J. Treacy, J.B. Higgins, Collection of Simulated XRD Powder Patterns for Zeolites, 5th edition, Elsevier, Amsterdam, 2007.
[34] S. Mintova, V. Valtchev, T. Onfroy, C. Marichal, H. Knözinger, T. Bein, Micropor. Mesopor. Mat. 90 (2006) 237–245.
[35] A. Corma, M. Moliner, Á. Cantín, M.J. Díaz-Cabañas, J.L. Jordá, D. Zhang, X. Zou, Chem. Mater. 20 (2008) 3218–3223.
[36] (a) D.S.A. Silva, W.N. Castelblanco, D.H. Piva, V. de Macedo, K.T.G. Carvalho, E.A. Urquieta-González, Mol. Catal. 492 (2020) 11026; (b) F. Jin, Y. Li, Catal. Today. 145 (2009) 101–107.
[37] K.Y. Nandiwale, P. Gogoi, V.V. Bokade, Chem. Eng. Res. Des. 98 (2015) 212–219.
[38] J. Liu, N. Ding, X. Hong, S. Zhou, X. Zhou, J.A. Wang, L. Chen, Catal. Lett. 150 (2020) 2996–3006.
[39] P. Schneider, P. Hudec, O. Solcova, Micropor. Mesopor. Mater. 115 (2008) 491–496.
[40] M.M.J. Treacy, J.B. Higgins, Collection of Simulated XRD Powder Patterns for Zeolites, 5th ed., Elsevier, Amsterdam, 2007.
[41] B.C. Lippens, J.H. de Boer, J. Catal. 4 (1965) 319–323.
[42] M. Thommes, K. Kaneko, A.V. Neimark, J.P. Olivier, F. Rodriguez-Reinoso, J. Rouquerol, K.S.W. Sing, Pure Appl. Chem. 87 (2015) 1051–1069.
[43] M. Tamura, K.-I. Shimizu, A. Satsuma, Appl. Catal. A: General 433-434 (2012) 135–145.
[44] C.-C. Chang, S. Cao, S. Kang, L. Kai, X. Tian, P. Pandey, R.B. Silverman, Bioorg. Med. Chem. 18 (2010) 3147–3158.
[45] D. Zhang, M. Sha, J. Chem. Res. 42 (2018) 141–144.
[46] K. Nakajima, Y. Zhang, Y. Nishibayashi, Org. Lett. 21 (2019) 4642–4645.